Dielectric Relaxation in Phase-Segregated Mixtures of Polystyrene and Liquid Crystal 5CB

Hironobu Hori, Osamu Urakawa, and Keiichiro Adachi*

Department of Macromolecular Science, Graduate School of Science, Osaka University, Toyonaka, Osaka 560-0043, Japan

Received September 24, 2003; Revised Manuscript Received November 10, 2003

ABSTRACT: Phase behavior and dynamics in blends of a liquid crystal 4-cyano-4′-*n*-pentylbiphenyl (5CB) and polystyrene(PS) were investigated by using dielectric spectroscopy. The blends exhibit phase separation of a UCST type. Below the phase-separation temperature, the blends separate into the isotropic PS-rich and 5CB-rich phases. With decreasing temperature the 5CB-rich phase transforms into the nematic liquid crystalline state and subsequently into the regular crystalline states. The nematic phase supercools about 30 K below the nematic-to-crystal transition point T_{NC}. Optical micrographs of blends indicate that spherical 5CB-rich domains are dispersed in the matrix of PS-rich phase even at the 5CB content of 80%. A strong dielectric relaxation due to rotation of the 5CB molecules in the isotropic PS-rich phase has been termed α. The α process exhibits complex temperature dependence due to the changes in the composition and morphology with temperature. Although the 5CB-rich phase crystallizes mostly at low temperatures, some 5CB-rich droplets of a small size remain without crystallization and exhibit dielectric relaxations termed β and γ. The β and γ processes are assigned to rotation of the 5CB molecules around the short and long axes of the rodlike 5CB molecule, respectively. Besides those dipolar relaxation processes, a relaxation termed α′ is observed at PS/5CB compositions of 5/5 and 4/6 and assigned to the Maxwell−Wagner effect.

Introduction

Many studies on the phase behavior and physical properties of polymer/liquid crystal (LC) blends have been reported.[1−16] Behaviors commonly seen in those blends are as follows. The phase diagram is of the upper-critical-solution-temperature (UCST) type. Below the binodal temperature, blends separate into two isotropic phases, and then, the LC-rich phase transforms into the nematic phase of almost pure 5CB. With further decrease of temperature the LC phase transforms into the regular crystalline phase. On the other hand, the polymer-rich phase remains in the isotropic state. Phase separation of polymer/LC blends having a suitable composition results in a morphology in which droplets of the liquid crystal (LC) are dispersed in the polymer matrix. Such blends are called "polymer-dispersed liquid crystal" (PDLC).[17−19] PDLCs are opaque under absence of an electric field but turn into a transparent material under an electric field due to matching of the refractive indices of the polymer and the oriented LC. Thus, PDLCs have been applied as optical devises.[17−19]

It is expected that irreversible effects such as supercooling and phase separation through binodal or spinodal decompositions cause formation of transient metastable states and morphologies. Dielectric spectra are sensitive for monitoring such changes of transient phases. In the present study we are interested in kinetic effects on the phase behavior and morphology. The dielectric information on blends of polymer and LC is important for practical applications of PDLC in view of switching time and energy dissipation due to dielectric loss. So far many dielectric studies are reported for low molecular weight LCs and liquid crystalline polymers[20] but only a few dielectric studies are reported on PDLC.[21−23] Williams et al. investigated in detail the dielectric response of a PDLC under an applied electric field.[21] Similar studies were reported by Jadzyn et al.[22] and Miyamoto et al.[23] In those studies immiscible polymer/LC blends were used, and hence their morphology was independent of temperature. As far as we know, the dielectric behaviors of polymer/LC blends exhibiting UCST have not been reported. Recently we reported the dielectric relaxation in blends of polystyrene (PS) and 4-cyano-4′-*n*-pentylbiphenyl (5CB) which is a LC having a structure of $C_5H_{11}-C_6H_4-C_6H_4-CN$.[24] There we carried out dielectric measurements on isotropic blends being interested in the dynamical heterogeneity. In the present study, we aim to examine the dielectric behavior of the PS/5CB blends with concentration of 5CB higher than 50% where the blends exhibit phase separation and liquid crystalline nature of 5CB becomes prominent. We focused our attention on the dynamics of the 5CB molecules in various phase-separated states and the transient behavior of the phase separation. To this aim, we also observed the morphology using a polarizing microscope.

Experimental Section

Materials. Polystyrene (PS) was synthesized by anionic polymerization with *sec*-butyllithium as the initiator. The weight-average molecular weight M_w and M_w/M_n ratio were determined to be 5.78×10^4 and 1.03, respectively, by using GPC (Tosoh, Tokyo, Japan). 5CB was purchased from Merck-Japan (Tokyo) and used without further purification. Blends were prepared as follows. Prescribed amounts of the components were dissolved in methyl ethyl ketone or benzene and then the solvent was removed under vacuum at 320 K. Four blends containing 49, 60, 80, and 91 wt % of 5CB were coded as PS/5CB(5/5), PS/5CB(4/6), PS/5CB(2/8), and PS/5CB(1/9), respectively.

Methods. The phase diagram was produced by using a polarizing optical microscope (Nikon E−400, Tokyo) and a

* Corresponding author. E-mail: adachi@chem.sci.osaka-u.ac.jp.

10.1021/ma035430z CCC: $27.50
Published on Web 01/21/2004

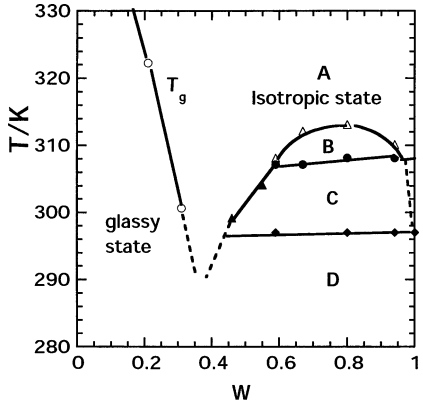

Figure 1. Phase diagram of the PS/5CB system. Phases A and B are the isotropic one-phase and two-phase regions, respectively. In the region C the isotropic PS-rich solution and liquid crystalline 5CB coexist. In the region D, the isotropic PS/5CB phase and 5CB crystalline state coexist. The open circles indicate T_g of the isotropic phase.

homemade light-scattering apparatus as reported previously.[24] A differential scanning calorimeter (DSC, SII SSC-580, Tokyo) was used for determination of T_g at the heating rate of 10 K/min. Dielectric measurements were carried out with an RLC meter (QuadTech 7600, Maynard, MA) over frequency range from 10 Hz to 2 MHz. The temperature dependence of the dielectric constant ϵ' and loss factor ϵ'' were measured at the rate of ±0.1 K/min.

Results and Discussion

Phase Diagram and Morphology. Figure 1 shows the phase-separation temperatures plotted against weight fraction w of 5CB. As previously reported, this system exhibits the phase diagram of an upper critical solution temperature type.[24] In region A, blends are in an isotropic single phase. The phase separation into two isotropic phases occurs in region B. The isotropic-to-nematic transition temperature T_{NI} of pure 5CB is 308 K. Below T_{NI}, the 5CB-rich phase transforms into an almost pure nematic 5CB phase and an isotropic PS-rich phase. The solid circles indicate the temperature at which the nematic phase appears when blends are cooled slowly. Thus, the isotropic PS-rich phase and the nematic 5CB phase coexist in the region C. The transition temperature of 5CB from the crystal to the nematic phase T_{CN} is 297 K. In the region D, the crystalline state is the most stable in the 5CB-rich phase. However, as described later, the nematic state is easily supercooled and the nematic phase crystallizes at a temperature far below T_{CN}. The open circles show glass transition temperatures T_g of the isotropic phases. The glass transition point of blend decreases from 373 K of pure PS with increasing content of 5CB indicating that 5CB acts as a plasticizer.

Figures 2 and 3 show the optical micrographs of PS/5CB(2/8) and PS/5CB(5/5), respectively. Observations were made by the cross-polarized mode in the cooling (a) and heating (b) directions at a rate of ±0.1 K/min. Observations in the heating direction were made after keeping the samples at 250 K for 5 h. As seen in Figure 2a. the field at 310 K is completely dark since the blend is composed of two isotropic phases. At 308 K, an anisotropic nematic phase appears due to the T_{NI} transition. Obviously the bright and dark regions are due to the 5CB-rich phase and PS-rich phase, respectively. In Figure 2a, the gradient of phase boundary is seen at 308 K. Below 302 K, the blend exhibits relatively

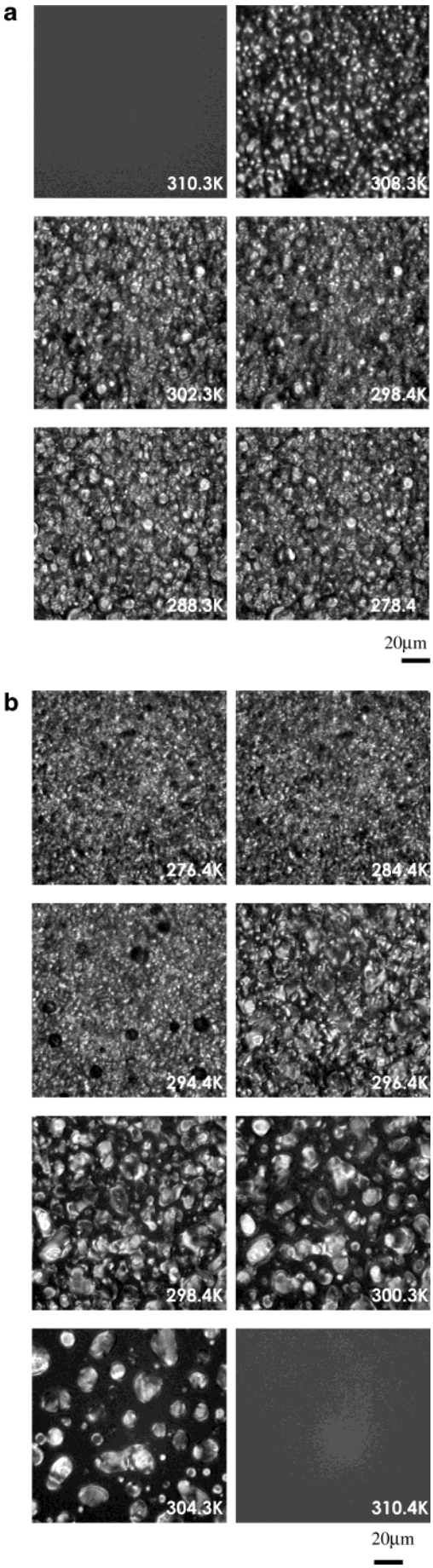

Figure 2. Polarizing micrographs of PS/5CB(2/8) measured in the cooling direction (a), and those in the heating direction (b).

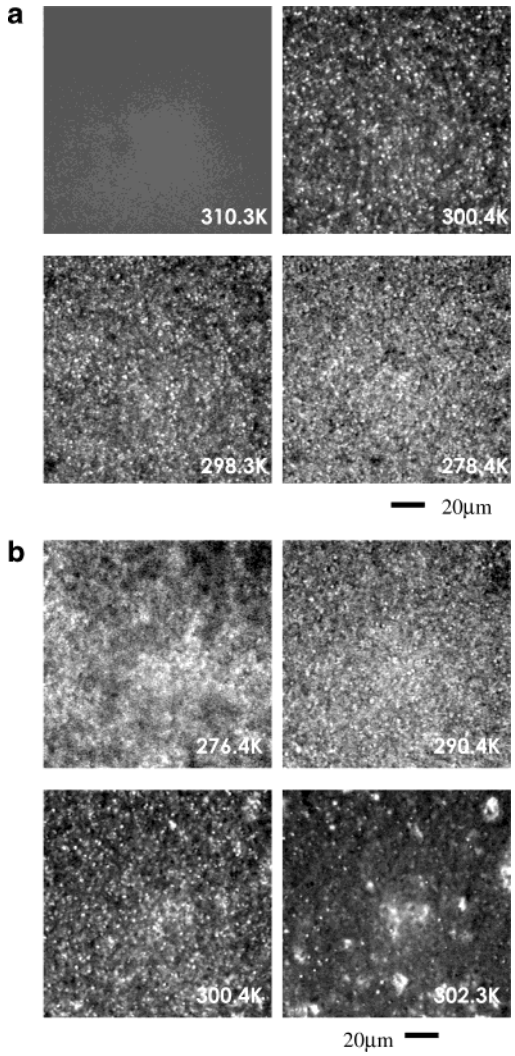

Figure 3. Polarizing micrographs of PS/5CB(5/5) measured in the cooling direction (a), and those in the heating direction (b).

sharp boundary. It is seen that spherical 5CB domains are surrounded by the isotropic phase. This morphology is kept down to 278 K.

Figure 2b shows the micrographs obtained in the heating course observed after annealing at 250 K for 5 h. We see that the domain size in the range below 294 K are different from those above 297 K. Since the transition temperature from the crystal to the nematic phase T_{NC} is 297 K, the blend is a mixture of the crystalline 5CB and isotropic PS-rich phase below 294 K. Above 298 K, the blend exhibits the morphology of the 5CB domains suspended in the PS-rich phase. It is seen that the 5CB domains observed in heating course is larger than those in cooling. We speculate the reason for this change as follows. As mentioned above observations in the heating direction were made after annealing at 250 K for 5 h. During this annealing process, further secondary crystallization took place. Therefore, the size of crystallites at about 275 K shown in Figure 2b are smaller than that seen in Figure 2a. Because of the crystallization at low temperature, the 5CB-rich domains coalesced when the crystalline phase transform into the LC phase. Thus, droplets are formed at about 300 K in the heating observation are larger than in cooling observation.

Both in parts a and b of Figure 2, we can recognize small bright domains especially in the photographs

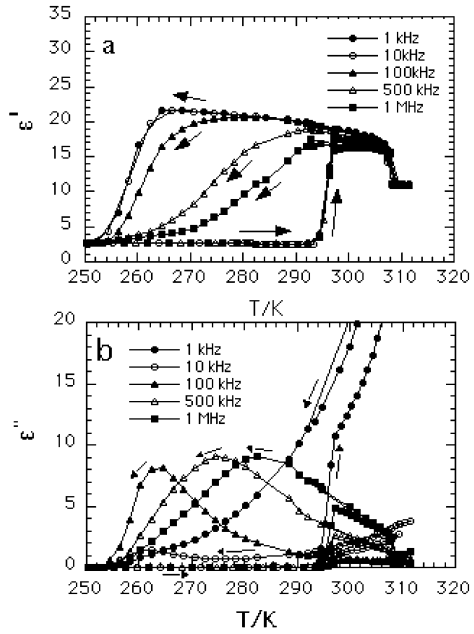

Figure 4. Temperature dependences of ϵ' (a) and ϵ'' (b) of pure 5CB measured in the cooling direction and subsequent heating at ±0.1 K/min. Arrows indicate the directions of temperature change.

below 294 K. The bright domain means that the phase is highly anisotropic and therefore those small domains can be assigned to the supercooled 5CB nematic phase which does not crystallize at low temperatures as will be indicated later for the dielectric data. However, we do not have evidence to support this assignment.

In the photographs of PS/5CB(5/5) shown in Figure 3, we see that the size of domains is much smaller than that observed in Figure 2. In the course of cooling (Figure 3a), the morphology is almost independent of temperature, but in the course of heating complicated structure is seen. This is again ascribed to the growth of crystalline 5CB domains during annealing at 250 K. Small bright domains are seen as observed for PS/5CB-(2/8) (Figure 2).

Dielectric Behavior of Pure 5CB. The dielectric behavior of pure 5CB was reported by Zeller[25] and Urban et al.[26] Zeller found that a thin layer (20 μm) of the nematic phase of 5CB is easily supercooled and exhibits glass transition at 210 K.[25] The temperature dependence of the dielectric relaxation time was expressed by the Vogel−Fulcher equation.[27,28] Urban et al. reported the dielectric behavior in the isotropic state of 5CB and 4-(2-methylbutyl)-4′-cyanobiphenyl.[26] Figure 4a shows the temperature dependence of the dielectric constant ϵ' of pure 5CB measured in the cooling direction at the rate of −0.1 K/min at various frequencies indicated in the figure. It is noted that the sample thickness was about 0.5 mm and hence the effect of thin layer was absent. At about 308 K (T_{NI}), ϵ' increases stepwise. We see that isotropic phase is hardly supercooled and that ϵ' in the nematic state is higher than the isotropic phase. By further cooling, ϵ' at 500 kHz and 1 MHz decreases gradually and the dielectric loss factor ϵ'' exhibits maximum (Figure 4b) due to dielectric dispersion. This indicates that the nematic phase is supercooled as reported by Zeller.[25] A similar decrease of ϵ' is seen around 260 K in the ϵ' curves at 1 and 10 kHz. However the behavior is different from that seen at high frequencies. The values of ϵ' are almost the

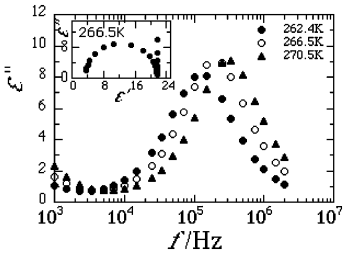

Figure 5. Frequency dependence of ϵ'' in the supercooled nematic state of pure 5CB and the Cole−Cole plot at 266.5 K (inset).

same, and the ϵ'' curves do not exhibit a maximum. From the frequencies of maximum ϵ'' at 500 kHz and 1 MHz, we expect that the dielectric dispersion at 1 kHz occurs at about 200 K. Thus, the decrease of ϵ' at low frequencies around 260 K is due to the irreversible transition from the nematic to crystalline state. The high value of ϵ'' at 1 kHz around 300 K is ascribed to ionic conduction. As is usually observed, it decreases monotonically with decreasing temperature.

After slow cooling to 190 K, the dielectric measurements were carried out in the heating direction as indicated by arrows in parts a and b of Figure 4. In contrast to the cooling measurements, the ϵ'' in the heating measurements are almost zero in the temperature range below T_{CN} (=297 K) indicating that there is no freedom of molecular motion in the crystalline state of 5CB. At T_{CN} the ϵ' and ϵ'' recover stepwise to the value of the nematic state. A discrepancy is seen in the values of ϵ' and ϵ'' above T_{CN} between the cooling and heating runs. This is probably due to the difference in the orientation of the 5CB molecules with respect to the electrodes of dielectric measurements.

Figure 5 shows the frequency dependence of ϵ'' of the supercooled nematic phase. The ϵ'' curve is narrow compared with that of polymers and close to the Debye curve. Reflecting this, the Cole−Cole plot at 265.5 K is close to a semicircle as shown in the inset.

Dielectric Behavior of PS/5CB(2/8). Figure 6a shows the ϵ' curves of PS/5CB(2/8) measured in the cooling and heating directions at the rate about ±0.1 K/min. We focus attention on the behavior of ϵ' changes at the transition temperatures, i.e., the isotropic phase-separation temperature T_{II}(=313 K), the transition temperature T_{NI} (=308 K) in the 5CB-rich phase, and the crystallization temperature T_{CN}(=297 K) of 5CB. No sudden change of ϵ' is seen at T_{II}(=313 K) as shown in the inset. Most likely, the phase separation takes place gradually through the spinodal decomposition, and therefore, no steplike change is seen in the ϵ' curve. Around 306 K, ϵ' decreases slightly and is ascribed to the transition T_{IN} from the isotropic to nematic phase in the 5CB-rich phase. Comparing this behavior with the change of ϵ' at T_{IN} in pure 5CB (Figure 4a), we see that the direction of the change is the reverse of pure 5CB. We speculate that the 5CB molecules locating near the surface of the domains in the nematic state are immobilized and hence exhibit lower ϵ' than pure 5CB as reported by Williams et al.[21] Below this temperature, ϵ' decreases steeply with decreasing temperature due to dielectric relaxation (α process). At 260 K, a sudden decrease of ϵ' is seen. This is ascribed to the crystallization of the nematic phase. With further decrease of temperature two dielectric dispersions termed β and γ occur.

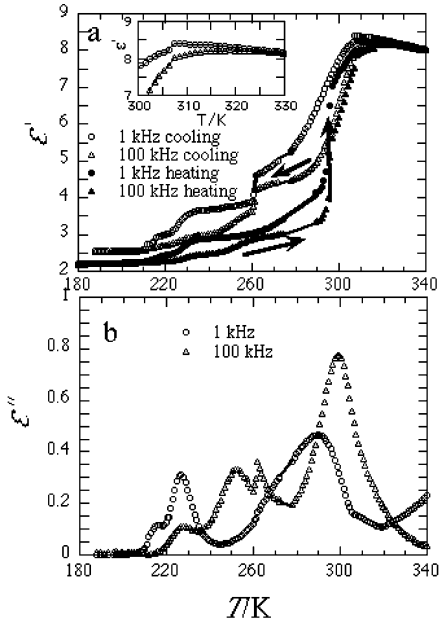

Figure 6. Temperature dependences of ϵ' and ϵ'' of PS/5CB-(2/8): (a) ϵ' measured in the cooling and subsequent heating directions; (b) cooling run for ϵ''. Arrows indicate the direction of cooling and heating at ±0.1 K/min.

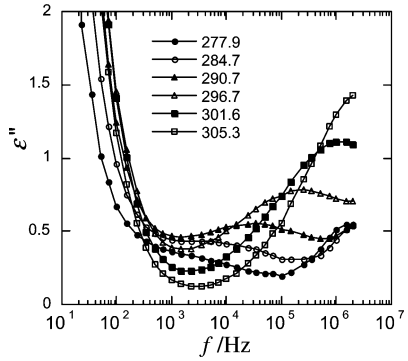

Figure 7. Frequency dependence of ϵ'' in PS/5CB(2/8).

In the heating curves the ϵ' values become smaller than the cooling curves indicating that the blend has crystallized further at low temperatures. We see that ϵ' increases at T_{CN} (297 K).

The corresponding ϵ'' curves measured in cooling direction are shown in Figure 6b. The heating curves are not shown here to avoid overcrowding. It is noted that as the dipole moment μ of 5CB is larger than that of the PS repeat unit by a factor of 17, the dielectric response ($\propto \mu^2$) of 5CB is ca. 290 times larger than PS. Therefore, the dielectric loss observed in this study reflects motions of the 5CB molecules.

Figure 7 shows the frequency dependence of ϵ'' measured in the cooling direction in the range between 280 and 305 K (the α process). The increase of ϵ'' below 100 Hz is due to ionic conduction. We expect that two relaxations appear in this temperature range: one is due to the 5CB-rich phase and the other to the PS-rich phase. However, from the Arrhenius plot of the loss maximum frequency for pure 5CB, the loss peak of the 5CB-rich phase locates above 1 MHz. Therefore, the broad loss peak (α) seen in this figure is ascribed to the PS-rich phase. Here we examine whether this assignment is consistent with the intensity of ϵ'' observed in Figure 7. From the tie lines on the phase diagram

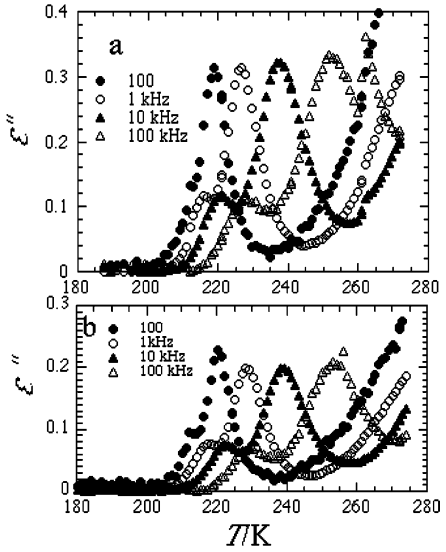

Figure 8. Temperature dependence of ϵ'' of PS/5CB(2/8) measured in the cooling (a) and subsequent heating (b) directions.

(Figure 1), the volume fraction of the PS-rich phase becomes 0.36 and the 5CB concentration 0.43 at 295 K. Thus, the intensity of the α process is expected to be 15% of that for pure 5CB. The height of the ϵ'' peak at 295 K is 0.8 and agrees in order with the expected intensity ($0.15 \times 9.0 = 1.4$). The slightly smaller intensity of the α process is due to the difference in the broadness of the ϵ'' curves. It is noted that T_g of the PS-rich phase is close to the temperature range used in Figure 7, and hence, the α relaxation is observed in the audiofrequency range.

It is seen that the intensity of the height of the loss peak decreases with decreasing temperature and at the same time the loss curves broaden. With decreasing temperature concentration of PS in the PS-rich phase changes along the binodal curve shown in Figure 1. We speculate that since temperatures are close to T_g, diffusions of the both components become slow and the equilibrium concentration is not attained locally. This results in the distribution of concentration and hence the distribution of the relaxation times.

Figure 8 shows the temperature dependences of ϵ'' in the temperature range where the β and γ relaxations are observed. Figures 8a and 8b were obtained in the cooling and subsequent heating measurements, respectively. It is noted that in this region the major phases are the crystalline 5CB and the glassy PS-rich phase. Since no dielectric relaxations corresponding to the β and γ processes are observed in either pure 5CB or blends of PS/5CB with the PS content higher than 60%,[24] these processes are due to a minor phase existing in the system.

Comparing parts a and b of Figure 8, we see again that the peak heights in the heating course become lower than those in the cooling course. This indicats that the loss peaks are due to a metastable state which disappears gradually with time. The frequency dependence of ϵ'' for the β and γ relaxations are plotted in Figure 9. The half-width of the β peak is about 1.3 decades and is close to the theoretical Debye curve. The Cole−Cole plot at 230.6 K for the β process (the arc of the right-hand side) is approximately semicircular indicating narrow distribution of relaxation times. In our previous dielectric studies on polymer/diluent systems, it was frequently observed that the secondary relaxations exhibited by diluents exhibited broad spectra with a width of approximately five decades.[24,29−31] Therefore, the β and γ relaxations cannot be assigned to the secondary relaxation in the PS-rich phase. Here it is noted that the nematic phase of pure 5CB exhibits quite narrow ϵ'' curve (Figure 5), and also the phase is easily supercooled. Therefore, we assign the β and γ processes to supercooled 5CB remaining in the system. As seen in Figure 2, there are many small bright domains assigned to the nematic phase. Most of the 5CB-rich phase transforms into the crystalline state but a small fractions of very tiny droplets of 5CB do not crystallize as reported by Zeller for thin film.[25] It is well-known that small drops such as water can be supercooled far below the melting temperature.[32]

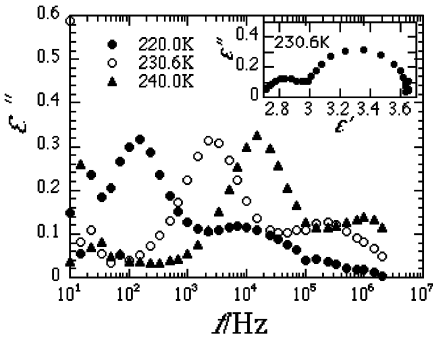

Figure 9. Frequency dependence of ϵ'' of PS/5CB(2/8) and the Cole−Cole plot at 230.6 K (inset).

Dielectric Behavior of PS/5CB(5/5). Parts a and b of Figure 10 show the temperature dependences of ϵ' and ϵ'' for PS/5CB(5/5) measured in the cooling direction. There are three ϵ'' peaks, and they are called α, β, and γ in order of decreasing temperature. From the phase diagram shown in Figure 1, we expect that PS/5CB(5/5) exhibits the phase separation at 302 K. In fact, Figure 3a clearly indicates the occurrence of the phase separation at this temperature. However, no appreciable change is seen in the ϵ' and ϵ'' curves. Slight changes in the slope of the temperature dependence curves of ϵ' and ϵ'' are seen at about 295 K as indicated by the dashed lines for the ϵ' curve at 1 kHz. Below this temperature the effect of the phase separation becomes prominent.

Figure 11 shows the frequency dependence of ϵ'' in the α relaxation region. We divide the temperature regions into regions above 295 (I) and below 295 K (II). In region I, the system exhibits broad ϵ'' curves which broadens with decreasing temperature. This behavior was also observed in Figure 7 for PS/5CB(2/8) and may be explained similarly. In region II, the ϵ'' curve become bimodal. We call the low-temperature peak the α′ process. The dielectric behavior of this process is abnormal: First this process does not exhibit a clear loss peak in the temperature dependence of ϵ'' shown in Figure 10. Second, the intensity increases rapidly with decreasing temperature. Furthermore, the α′ peak is narrower than the α process. Those behavior of the α′ process are much different from those in the isotropic PS/5CB(7/3) reported previously in ref 24 with respect to the broadness and the temperature dependence of intensity.

We tested whether the loss maximum frequency f_m of the α′ process can be explained in terms of the Maxwell−Wagner theory,[33,34] i.e., conductive drops are dispersed in a dielectrics. The simplest assumption is

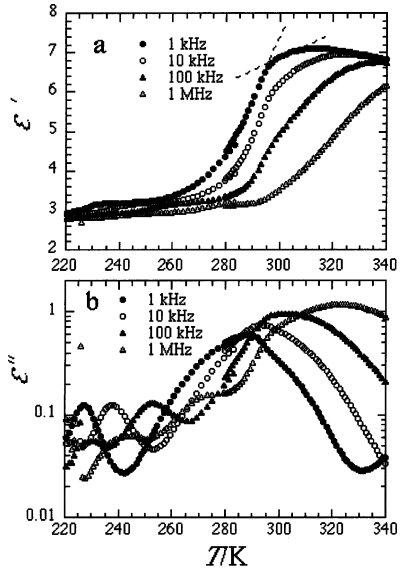

Figure 10. Temperature dependences of ϵ' (a) and ϵ'' (b) of PS/5CB(5/5) measured in the cooling direction.

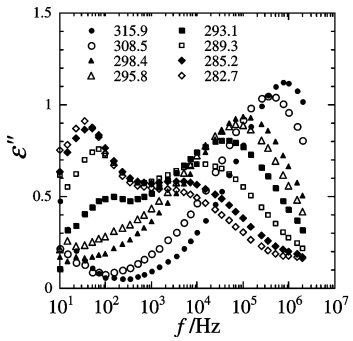

Figure 11. Frequency dependence of ϵ'' in PS/5CB(5/5).

the Maxwell model which assumes lamellae of an insulator phase 1 and a conductive phase 2 are placed perpendicular to an electric field. The relaxation time τ is given by

$$\tau = \epsilon_o \frac{\phi(\epsilon_1 + \epsilon_2) + \epsilon_2}{(1 + \phi)\sigma_2} \quad (1)$$

where ϵ_o, ϵ, and σ are the absolute dielectric constant of vacuum, the dielectric constant, and the conductivity, respectively and ϕ is the volume fraction of the phase 2. In the present PS/5CB(5/5) system, the nematic 5CB droplets correspond to the phase2 and the PS-rich phase to the phase 1. From the phase diagram shown in Figure 1, ϕ at 282 K is about 0.2. We estimate σ_2 as follows. In Figure 5, it is seen that ϵ'' increases with decreasing frequency in the range below 10^4 Hz. This is due to ionic conduction. The conductivity σ_2 is determined to be 3.22×10^{-9} S m^{-2} at 282 K. We estimate ϵ_1 and ϵ_2 to be about 5 and 21, respectively, from Figures 6 and 4. Then we obtain $\tau = 0.060$ s and $f_m = 2.7$ Hz which is about one order smaller than the observed f_m for the α' process at 282.7 K. Wagner calculated τ for a system in which a small amount of spherical drops (phase 2) are dispersed in an insulator (phase 1). The τ due to interfacial polarization of drops is given by

$$\tau = \frac{(2\epsilon_1 + \epsilon_2)\epsilon_0}{\sigma_2} \quad (2)$$

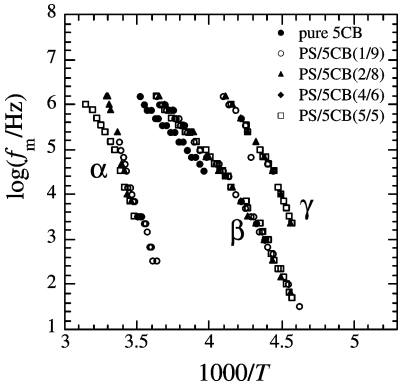

Figure 12. Arrhenius plots for the α, β, and γ processes of blends and pure 5CB.

From the data mentioned above, f_m due to the Wagner mechanism is calculated to be 2.3 Hz which is similar to the value obtained with eq 1. These results are rather subtle for judging whether the α' process is attributable to the Maxwell−Wagner effect since the value of σ_2 changes logarithmically depending on the content of impurity ions. We used σ_2 of pure 5CB in eqs 1 and 2 but the value in the drops formed by phase separation might be higher than that in pure 5CB. We consider tentatively that the α' process is due to the Maxwell−Wagner effect. More sophisticated theory was given by Bottcher[33] on the basis of the mean field approximation. Unfortunately the relaxation time or ϵ'' of heterogeneous systems cannot be expressed in terms of the analytical equations.

Now we examine the behavior of the β and γ processes of PS/5CB(5/5). Comparing the peak positions of the β and γ processes between PS/5CB(5/5) and PS/5CB(2/8) (Figures 8 and 10), we see that the peak positions are the same. Moreover the frequency dependence curves of ϵ'' for the β and γ processes are quite narrow as seen for PS/5CB(2/8). Therefore, the β and γ processes observed for PS/5CB(5/5) can be assigned to the motions of the 5CB molecules in supercooled 5CB droplets as assigned for PS/5CB(2/8). This is confirmed by the micrograms shown in Figure 3, where tiny bright domains can be seen.

Dielectric Behavior of PS/5CB(1/9) and PS/5CB-(4/6). The dielectric behavior in PS/5CB(2/8) and PS/5CB(5/5) have been described above. Blends with intermediate compositions, i.e., PS/5CB(1/9) and PS/5CB(4/6), also exhibited the α, β, and γ relaxations similarly to PS/5CB(2/8) and PS/5CB(5/5). For PS/5CB-(4/6) the α' process was also observed. Although the intensity and the loss peak temperature differ from sample to sample, the qualitative behaviors of all blends investigated in this study are very similar. So far we assumed that the β process is due to droplets of 5CB in the PS-rich phase. It is rather surprising that PS/5CB-(1/9) also forms such a morphology. We speculate that small droplets of 5CB are also formed in the PS-rich phase at low temperature.

Arrhenius Plot. Figure 12 shows the Arrhenius plots of the PS/5CB blends and pure 5CB where the loss maximum frequencies f_m are plotted against the inverse of temperature. It is noted that since the composition of the PS-rich phase is given by the phase diagram, the values of f_m for the α, β, and γ processes should be independent of the PS/5CB blending ratio in the equilibrium states. Therefore, it is expected that the Arrhenius plots for blends having different compositions lie

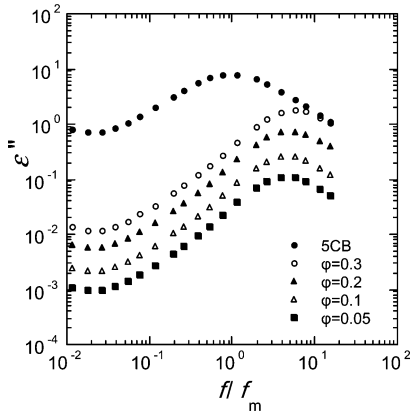

Figure 13. ϵ'' curves calculated with eq 3 for the case where the spherical 5CB droplets are suspended in a matrix with $\epsilon' = 2.8$. ϕ represents the volume fraction of the 5CB drops.

on the same curve if the phaseseparated state is in equilibrium but do not if the blends are in nonequilibrium states. In Figure 12, we see that the plots for the α processes of blends with different compositions do not lie on a common curve. This indicates that some blends are in nonequilibrium states. It is reminded that dielectric measurements were made at the cooling or heating rate of ±0.1 K/mim. This condition is not slow enough to achieve equilibrium concentration in the PS-rich phase.

In Figure 12, we see that the plots for the β process of blends locate close to the plots of pure 5CB. This supports the assignment of the β peak mentioned above. However, we see that the curve for the β process of blends locates at slightly higher frequency than pure 5CB. This is explained by the effect of heterogeneous structure of the system as follows. According to Wagner,[34] the complex dielectric constant ϵ^* of a heterogeneous system in which spherical drops are dispersed in a matrix is generally given by

$$\epsilon^* = \epsilon_1^* \frac{2\epsilon_1^* + \epsilon_2^* - 2\phi(\epsilon_1^* - \epsilon_2^*)}{2\epsilon_1^* + \epsilon_2^* + \phi(\epsilon_1^* - \epsilon_2^*)} \qquad (3)$$

where $\epsilon_1^*(=\epsilon_1 - i\epsilon_1'')$ and $\epsilon_2^*(=\epsilon_2 - i\epsilon_2'')$ are the complex dielectric constants of the matrix and the drop, respectively, and ϕ is the volume fraction of the drop phase. The theory assumes that $\phi \ll 1$ which is compatible with the present system because the fraction of LC drops at low temperature is small. In the previous section we attempted to explain the α′ process using the Maxwell−Wagner model. In the discussion of this section, the conductivity does not play important role, since the β and γ relaxations occur in low-temperature region. In such a situation, eq 3 predicts the dielectric behavior of the heterogeneous system. Equation 3 was calculated by using the numerical data of the present blend and plotted in Figure 13. Here the loss part of ϵ_1 is neglected and ϵ_1' is taken to be 2.8 since the PS-rich phase forming the matrix phase is in the glassy state at temperatures where the β process is observed. For ϵ_2^*, the complex dielectric constant of the nematic phase of pure 5CB plotted against the reduced frequency f/f_m was used since the exact f_m of pure 5CB at low temperatures is not available.

As is seen in Figure 13, the loss peak of the heterogeneous system locates at higher frequency than pure 5CB. Comparing the loss peak heights ϵ''_{max} of pure 5CB and the blend, we note that the ϵ''_{max}(blend) is much lower than $\phi\epsilon''_{max}$(5CB). From the values of the calculated ϵ''_{max} shown in Figure 13, we estimate that ϕ of the supercooled nematic droplets of 5CB is 0.11 for PS/5CB(2/8) and $\phi = 0.051$ for PS/5CB(5/5).

In Figure 12, the Arrhenius plot for the γ process is almost parallel to that for the β process indicating that the γ process is also due to the supercooled 5CB. We cannot see this process in Figure 5 due to the limited frequency range. Existence of two modes in nematic LCs has been reported by several authors:[35−37] the main peak is assigned to rotation of the rodlike LC molecules around the axis perpendicular to the rod and the side peak due to rotation around the axis parallel to the rod-LC molecule. Threfore the β and γ processes can be assigned to rotation of the 5CB molecules around the short and long axes, respectively. The activation energy for the γ process is higher than that for the β process. Ghanadzadeh and Beevers[36] studied the dielectric response of a mixture of nematic LCs and reported the similar behavior. They explained the difference of the activation energy by considering the temperature dependence of the molecular packing in the supercooled state. The same mechanism may be applicable to 5CB.

Conclusion

We have examined the dielectric behavior of phase-segregated PS/5CB blends. The phase diagram of this system is a UCST type and the critical temperature and composition are 313 K and 80% of the 5CB content, respectively. Three phases appear depending on composition and temperature, i.e., isotropic PS/5CB mixture, almost pure 5CB nematic state, and the crystalline 5CB. Morphologies of the blends observed by a polarizing microscope change at those transition temperatures. It is found that 5CB phase supercools below the crystal−nematic transtion temperature T_{NC} and some small 5CB domains do not crystallize even at temperatures far below T_{NC}. Those small 5CB domains can be observed as small bright domains in the micrographs. By dielectric measurements, it is found that transitions among those phases result in sudden changes of dielectric constant ϵ' and the loss factor ϵ''. There are three ϵ'' peaks termed α, β, and γ in the phase-separated samples. The α process originates from motions of 5CB in the isotropic PS-rich phase. The Arrhenius plots for the α process of blends with various compositions do not lie on a common curve indicating that blends are in a nonequilibrium state. For PS/5CB(5/5) and (4/6), another relaxation process termed α′ is observed and has been assigned tentatively to the Maxwell−Wagner effect. The β and γ processes are due to motions of the 5CB molecules in domains of the supercooled nematic phase and are assigned to rotation of the 5CB molecules around the short and long axes of the rod like 5CB molecules.

Acknowledgment. H.H. thanks the Suzuki Foundation for a scholarship.

References and Notes

(1) Roussel, F.; Canlet, C.; Fung, B. M. *Phys. Rev. E* **2003**, *65*, 021701.

(2) Roussel, F.; Buisine, J.-M.; Maschke, U.; Conqueret, X. *Phys. Rev. E* **2003**, *62*, 2310.

(3) Silimane, S. K.; Maschke, U.; Benmouna, F.; Bacquet, M.; Roussel, F.; Buisine, J.-M.; Conqueret, X.; Benmouna, M. *Eur. Polym. J.* **2002**, *38*, 461.

(4) Bouchaour, T.; Benmouna, F.; Roussel, F.; Buisine, J.-M.; Conqueret, X. Benmouna, F.; Maschke, U. *Polymer* **2001**, *42*, 1663.
(5) Borrajo, J.; Riccardi, C. C.; Williams, R. J. J.; Siddiqi, H. M.; Dumon, M.; Pascault, J. P. *Polymer* **1998**, *39*, 845.
(6) Matsuyama, A.; Kato, T. *J. Chem. Phys.* **2000**, *112*, 1046.
(7) Matsuyama, A.; Kato, T. *Phys. Rev.* **1999**, *59*, 763.
(8) Zhu, J.; Xu, G.; Ding, J.; Yang, Y. *Macromol. Theory Simul.* **1999**, *8*, 409.
(9) Lin, Z.; Zhang, H.; Yang, Y. *Macromol. Chem. Phys.* **1999**, *200*, 943.
(10) Lin, Z.; Zhang, H.; Yang, Y. *Phys. Rev.* **1998**, *58*, 5867.
(11) Patwardhan, A. A.; Berfiore, L. A. *Polym. Eng. Sci.* **1998**, *28*, 916.
(12) Chiu, H.-W.; Kyu, T. *J, Chem. Phys.* **1999**, *110*, 5998.
(13) Shen, C.; Kyu, T. *J, Chem. Phys.* **1995**, *102*, 556.
(14) Lin, Z.; Zhang, H.; Yang, Y. *Macromol. Theory Simul.* **1997**, *6*, 1153.
(15) Yang, Y.; Lu, J.; Zhang, H.; Yu, T. *Polym. J.* **1994**, *26*, 880.
(16) Ahn, W.; Kim, C. Y.; Kim, H.; Kim, S. C. *Macromolecules* **1992**, *25*, 5002.
(17) Doane, J. W.; Vaz, N. A.; Wu, B. G.; Zumar, S. *Appl. Phys. Lett.* **1986**, *48*, 269.
(18) Vaz, N. A.; Smith, G. W.; Montgomery, G. P., Jr. *Mol. Cryst. Liq. Cryst.* **1987**, *146*, 17.
(19) West, J. L. *Mol. Cryst. Liq. Cryst.* **1988**, *157*, 427.
(20) Williams, G. In *Molecular Dynamics of Liquid Crystals*; Luckhurst, G. R., Veracini, C. A., Ed.; Kluwer Academic: Dordrecht, The Netherlands, 1994; p 431.
(21) Williams, G.; Shinton, S. E.; Aldridge, G. A. *J. Polyn. Sci. B: Polym. Phys. Ed.* **2001**, *39*, 1173.
(22) Jadzyn, J.; Czechowski, G.; Mucha, M.; Nastal, E. *Liq. Cryst.* **1999**, *26*, 453.
(23) Miyamoto, A.; Kikuchi, H.; Kobayashi, S.; Morimura, G.; Kajiyama, T. *Macromolecules* **1991**, *24*, 3915.
(24) Hori, H.; Urakawa, O.; Adachi, K. *Polym. J.* **2003**, *35*, 721.
(25) Zeller, H. R. *Phys. Rev. Lett.* **1982**, *48*, 334.
(26) Urban, S.; Gestblom, B.; Dabrowski, R. *Phys. Chem. Chem. Phys.* **1999**, *1*, 4843.
(27) H.Vogel, H. *Phys. Z.* **1921**, *22*, 645.
(28) Fulcher, G.A. *J. Am. Ceram. Soc.* **1925**, *8*, 339.
(29) Yoshizaki, K.; Urakawa, O.; Adachi, K. *Macromolecules* **2003**, *36*, 2349.
(30) Yada, M.; Nakazawa, M.; Urakawa, O.; Morishima, Y.; Adachi, K. *Macromolecules* **2000**, *33*, 3368.
(31) Nakazawa, M.; Urakawa, O.; Morishima, Y.; Adachi, K. *Macromolecules* **2000**, *33*, 7898.
(32) Rosenfeld, D.; Woodley, W. L. *Nature (London)* **2000**, *405*, 440.
(33) Bottcher, C. J. F.; Bordewijk, P. *Theory of Electric Polarization Vol. II*; Elsevier: New York, 1978; pp 476−487.
(34) Wagner, K. W. *Arch. Electrotech.* **1914**, *2*, 378.
(35) Bose, T. K.; Chahine, R.; Merabet, M.; Thoen, J.: *J. Phys. (Paris)* **1984**, *45*, 1329.
(36) Ghanadzadeh, A.; Beevers, M. S. *J. Mol. Liq.* **2001**, *94*, 97.
(37) Nozaki, R.; Bose, T. K.; Yagihara, S. *Phys. Rev. A* **1992**, *46*, 7733.

MA035430Z